Applied Physics Letters

RESEARCH ARTICLE | MAY 09 2023

Ultrafast low-jitter optical response in high-temperature superconducting microwires

A. Kumar; D. Panna; S. Bouscher; ... et. al

Appl. Phys. Lett. 122, 192604 (2023)
https://doi.org/10.1063/5.0150805

AIP Publishing

Applied Physics Letters ARTICLE pubs.aip.org/aip/apl

Ultrafast low-jitter optical response in high-temperature superconducting microwires

Cite as: Appl. Phys. Lett. **122**, 192604 (2023); doi: 10.1063/5.0150805
Submitted: 16 March 2023 · Accepted: 25 April 2023 ·
Published Online: 9 May 2023

A. Kumar,[1] D. Panna,[1] S. Bouscher,[1] A. Koriat,[1] Y. Nitzav,[2] R. Jacovi,[1] A. Kanigel,[2] and A. Hayat[1,a)]

AFFILIATIONS

[1]Department of Electrical Engineering, Technion Israel Institute of Technology, Haifa 3200003, Israel
[2]Department of Physics, Technion Israel Institute of Technology, Haifa 3200003, Israel

[a)]Author to whom correspondence should be addressed: alex.hayat@ee.technion.ac.il

ABSTRACT

We report ultrafast optical response in high-T_c superconductor ($YBa_2Cu_3O_{7-\delta}$) based microwires operating at 76 K and we find a rise time ~850 ps and a fall time ~1250 ps and an upper limit of timing jitter of ~100 ps, using twice the standard deviation of the fitted data. In our experiment, incident power is proven to be an important factor for a device jitter. At low incident power, a lower rate of hot-spot generation by a smaller number of absorbed photons results in a longer latency time to obtain the required number of hot-spots for superconductor-to-normal transition. The lower hot-spot generation rate also results in larger timing jitter of the device. Whereas, at high incident power, a higher hot-spot generation rate yields shorter latency and smaller timing jitter. These observations agree well with our statistical model. Enhancing the sensitivity of the current device can enable future high-T_c superconductor nanowire single photon detectors, toward the widespread use of ultrafast quantum technologies.

A wide range of technological and scientific fields, such as astronomy, medical imaging, and optical quantum information science, rely on the ability to detect low-intensity optical radiation down to single-photon sensitivity spanning a wide wavelength range.[1–3] Single-photon detectors have enabled and supported many applications including time-of-flight measurement in laser ranging and ground-space communication, spectroscopy of atoms and molecules, time-correlated single photon detection for quantum light source characterization, and even in studies of the dark matter.[4–7] In the past two decades, superconductor nanowire single photon detectors (SNSPDs) have been tremendously developed and technologically matured. Since their inception, they compete with conventional detectors based on photo-multiplier tubes and semiconductor avalanche photodiodes.[8] Due to the small superconducting gap, photons in visible and infrared ranges can be detected using the same superconducting film. This is particularly attractive when no suitable detectors exist for the wavelengths of interest. The SNSPDs offer high quantum efficiencies in both visible and infrared wavelengths, low dark current rates, fast time response with short dead time, extremely small timing jitter, and, in certain cases, ability to resolve photon numbers.[9–11] Many research fields of the optical quantum information science have successfully integrated SNSPDs into their measurement facilities further stimulating improvements of these detectors. Long-range quantum key distribution applications heralded single-photon and entangled light source characterization all benefit from the highly efficient SNSPDs operating at the telecom and infrared wavelengths.[12] Timing resolution becomes crucial for many applications such as the accurate determination of the arrival time of a photon which limits the security of quantum key distribution.[13] The timing jitter also sets the resolution in time-of-flight laser ranging (LIDAR).[4] The main disadvantage of the already existing SNSPDs based on low-T_c superconductors is the requirement for liquid He cooling which makes them less technologically affordable in the industry. One possible solution is to use superconductors operating at the boiling temperature of liquid nitrogen—a practical coolant found in many infrared sensing applications. These high-T_c superconductors recently drew the attention of the engineering and scientific community as candidates enabling SNSPD technology to a wide variety of industry domains. Cuprate based superconductor photon detectors despite having the high-T_c have remained unexplored. The technological challenge of producing nanowires of high-T_c superconducting films is one issue. Charaev *et al.*[14] recently demonstrated SNSPDs fabricated out of two high-T_c cuprate superconductors, $Bi_2Sr_2CaCu_2O_{8+\delta}$ (BSCCO) and $La_{2-x}Sr_xCuO_4$ (LSCO), which exhibit a single-photon response up to 25 and 8 K, respectively.

Here, we report ultrafast response from $YBa_2Cu_3O_{7-\delta}$ (YBCO, a cuprate-based high-temperature superconductor) based microwire at

76 K, fabricated using our selective epitaxial growth (SEG) method and electron-beam lithography technique.[15] We investigate the timing jitter of our detector, which is a highly important practical characterization for various applications. We show the transient response of the microwire when excited with a 4 ps pulsed light from a titanium sapphire laser. The measurements show an ultrafast rise and fall time ~850 and ~1250 ps, respectively, and ~100 ps timing jitter operating at 76 K. The experimental studies show that our device jitter depends on the incident power and exhibits minimum jitter when the power is maximal. When the incident power is low, the fewer photons absorbed in the superconducting microwire lead to a slower rate of hot-spot generation, resulting in a longer time to get the necessary hot-spot number for the transition from superconducting to normal. This slower hot-spot generation also results in more timing jitter in the device. Conversely, when the incident power is high, the higher rate of hot-spot generation results in a shorter latency and lesser timing jitter. These outcomes agree with our statistical model.

To demonstrate the high-T_c based detector, we fabricated our devices using the SEG method. First, we deposited a thin film of Si_3N_4 (~30 nm) on a strontium titanate (STO) substrate using plasma assisted chemical vapor deposition technique. In the next step, we patterned the Si_3N_4 film using electron beam lithography. The exposed region of PMMA is dissolved using a solution of IPA:MIBK (1:3). The patterned regions of Si_3N_4 are etched using a reactive ion etching technique. In the end, a 50 nm thin YBCO film was deposited using pulsed-laser deposition (PLD). The details of the YBCO thin film fabrication have been reported elsewhere.[16] The benefit of this process is that the YBCO film is grown in the last step of the fabrication avoiding any chemical processing and preventing degradation of the superconducting film. Resulting YBCO that grows on the substrate remains crystalline and maintains its superconducting properties. This SEG process allows us to obtain microscale features without degrading the superconducting properties of the YBCO film.[17,18]

We characterize the superconducting properties by resistance vs temperature $R(T)$ and I–V measurements using a current source. First, the critical temperature of superconducting microwire was determined using the $R(T)$ measurement in the four-probe geometry. The measured resistance of the 9 μm width wire is shown in Fig. 1. On cooling the sample, we observe the onset of superconducting transition which is characterized by a drop in resistance when the temperature is below the critical temperature of $T_c \sim 81.5$ K. We performed the I–V measurement to extract the critical current densities at various temperatures and obtained the typical values of $J_c = 1$ MA/cm^2 at 77 K for the wire—consistent with the reported values for YBCO.[19–23] The relatively high critical current density value suggests the good quality of the PLD-grown microwires. We have neither done over doping nor introduced any pinning center in our YBCO film to further improve the critical current density as have been shown in some previous works.[24,25] A scanning electron microscope (SEM) image of our superconducting microwire device with current leads and pads (partially shown) is shown in the inset of Fig. 1.

The optical studies were performed in a liquid He closed-cycle cryogenic system with optical access to the sample. We used 4 ps-long, 82-MHz-repetition-rate pulses at 810 nm wavelength from a mode-locked titanium–sapphire laser as an optical excitation. The laser is focused to a spot size of about ~20 μm diameter and illuminates the $9 \times 20\ \mu m^2$ microwire area. Throughout the measurement, the

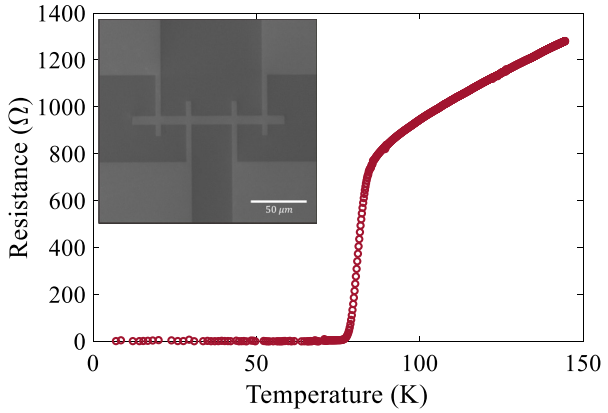

FIG. 1. Resistance as a function of temperature measurement of the 50 nm thin YBCO microwire epitaxially grown on STO substrate using a SEG method. The superconducting transition temperature is $T_c \sim 81.5$ K. Inset shows the SEM image of a 9 μm width microwire. The light and dark gray region corresponds where superconducting YBCO film and insulating film (on Si_3N_4 thin film) will grow, respectively.

microwire was dc current biased while maintaining the current and temperature below their critical values. The sudden transition from superconducting to the normal state generates a transient voltage pulse across the microwire.[3] It is important to note that the width of our device is 9 μm, and it requires several hot-spots to create a normal region across the width of the wire. The resulting voltage signal was amplified using a room-temperature rf amplifier with 1 GHz bandwidth and recorded on a digital oscilloscope. The detector response was measured at different bias currents (I_B), wire temperatures, and incident laser powers. The surface plot (Fig. 2) shows the microwire peak voltage as a function of bias current and temperature for a fixed incident average laser power of 15 mW.

The critical current values as a function of temperature are depicted with a star (☆) symbol and superimposed on top of the

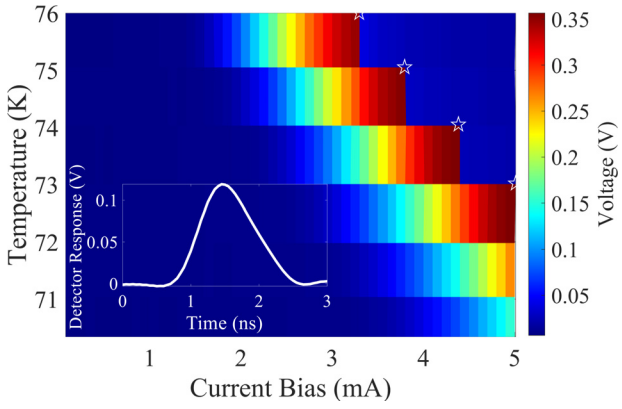

FIG. 2. Surface plot of voltage vs current at different temperatures. ⋆ shaped data points are critical currents obtained from $I(V)$ measurement. The inset shows the transient photoresponse of the detector recorded using a 1 GHz sampling oscilloscope when the wire was biased at 2.1 mA at 76 K and illuminated with 4 ps-wide, 82-MHz-repetition-rate pulses at 810 nm wavelength from a mode-lock titanium-sapphire laser.

surface plot. At low temperatures ($T < T_c$), the voltage response monotonically increases with the bias current, as expected. Although this increase in voltage response is limited by the wire critical current (Fig. 2). We observe in Fig. 2 that the response vanishes as it reaches the I_c because the superconducting wire becomes normal due to the applied bias current and incident light which drives the wire into the normal region. The inset of Fig. 2 shows the voltage pulse shape of our superconducting microwire detector, which indicates the detection event when the wire was biased close to the critical current ($I_B = 2.1$ mA at 76 K) and illuminated with an incident average power of 15 mW.

In the inset of Fig. 2, we observed a signal pulse with an amplitude of 0.12 V. The actual voltage pulse from the wire may be shorter in time than the measured one. It is noticeable from the inset of Fig. 2 that the rise time is ~850 ps and the fall time is ~1250 ps. These values are upper limit as it is limited primarily by the bandwidth of the amplifier used of 1 GHz.

One of the important metrics for any photon detector is the timing jitter which was characterized using a time tagger module with the "start" channel triggered by the low jitter fast photodiode (jitter < 2 ps) operating at laser repetition rate and indicating photon arrival at the sample while the amplified microwire signal was connected to the "stop" channel. The histogram of the time intervals between the start and stop channels was recorded, and twice the standard deviation (2σ) obtained by fitting the data is reported as the detector jitter in Fig. 3(a). The variation of timing jitter with respect to different incident average power of photons when biased with 1.7 mA current at 76 K is shown in Fig. 3(a) with the fitting of the data. From Fig. 3(a), it is noted that the timing jitter is sensitive to the incident laser power. We observe that jitter in Fig. 3(a) and latency values in Fig. 3(b) are higher at lower power compared to the values at large power incident on the wire.

To explain our experimental results, we present a statistical model of the physical mechanism underlying the operation of the detection and pulse generation of the device once the incident photons have been absorbed in the microwire. In our calculations, we assume that the voltage pulse appears after a certain number of hot-spots, N_0, is generated. Denoting the time of the voltage pulse generation T—a random variable—its distribution can be obtained by finding within what time duration the N_0^{th} hot-spot was generated.

We assume that the generation of hot-spots is a stochastic process, with time between consecutive events distributed exponentially $T_i \sim \mathrm{Exp}[\lambda]$, where λ is a rate parameter for hot-spot generation. In the experiment, we have a large number of events (hot-spots) and since time events are distributed exponentially, so the distribution of total time of a number of events is $T \equiv \sum_i T_i \sim E[N_0, \lambda]$, where E denotes the Erlang distribution.[26] For a sufficiently large N_0, the Erlang distribution approaches a normal distribution $\mathcal{N}\left[\frac{N_0}{\lambda}, \frac{N_0}{\lambda^2}\right]$. Based on this model, we have used a Gaussian fit for the distribution of counts vs time. This fit serves as an estimator for the distribution of the random variable T. This fit was done for each laser power and the experimental and theoretical jitter surface plots are shown in the upper and lower panels of Fig. 4, respectively.

We extracted two parameters from the calculations: the mean (μ) and standard deviation (σ). According to our calculations, we find a dependence of $\sigma \sim 1/N$ and $\mu \sim 1/N$, where N is the number of

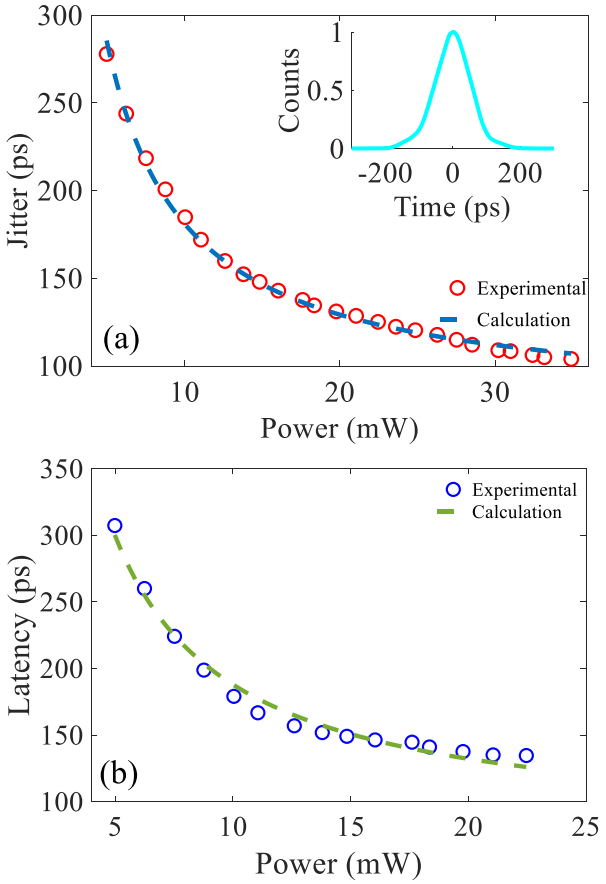

FIG. 3. (a) Main panel shows the measured jitter plot vs average laser power at a 1.7 mA bias current and the temperature was 76 K. The dashed curve is calculated dependence showing $\frac{1}{Power}$ behavior. The inset shows the histogram of the timing jitter of our device at a 1.7 mA bias current, 76 K temperature, and at 35 mW applied power. Twice the standard deviation obtained by fitting the measured data are ~100 ps. (b) Latency (mean arrival time) vs average power also with $\frac{1}{Power}$ behavior (dashed line).

hot-spots generated per unit time which is proportional to the number of absorbed photons per pulse, and thus, to the laser power P. This experimental result is predicted by our model: since λ is a rate parameter for hot-spot generation, and we assume it to be proportional to the number of photons. Also, for Gaussian distribution $\sigma = \frac{\sqrt{N_0}}{\lambda}$, the jitter σ should follow the same dependence on laser power as the latency T. In the inset of Fig. 3(a), we have shown the histogram plot of count vs time and by fitting these data with our model we found the standard deviation is ~100 ps at 35 mW average power and taken at 810 nm wavelength for our device. It is important to note that our time-tagger instrument has a lower limit of time resolution of ~100 ps. Hence, we are reporting the upper limit of the timing jitter of our device which is ~100 ps while the photodiode jitter is <2 ps. We also note in Figs. 3(b) and 4 that the latency is shifted in time depending on the incident power value which can be explained by our model. At lower power, it takes more time for the microwire to become normal leading to an overall increase in the timing jitter, and the latency timing increases as

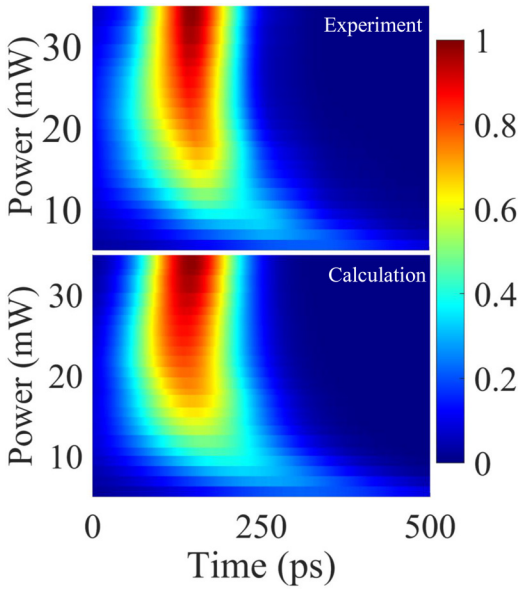

FIG. 4. Top (experimental) and bottom panel (calculated) are the jitter surface plots showing the voltage generation time probability distribution, at different incident average power. Normalized experimental statistics of distribution, similar to the probability distribution (theoretical).

it takes a longer time to generate the required number of hot-spots. At higher power, the transition to a normal state is more rapid due to a higher rate of hot-spot generation.

In our study, we have presented a model for microwire which does not include the interactions between hot-spots. We explained the generation of voltage pulse by requiring a certain number of hot-spots for the pulse generation, resulting in the pulse generation time statistics given by Erlang distribution. For nanoscale wires and smaller number of photons, a more sophisticated model by Akhlaghi and Majedi[27] including interaction between hot-spots is required. That model demonstrates that nanowires can respond to a small number of photons, with the response time decreasing with the increasing number of photons. In our microwire model, the response time diverges for a small number of photons (Fig. 3), due to the micrometer width of the wire preventing interactions between a small number of hot-spots.

In conclusion, we demonstrated an ultrafast high-temperature superconductor-based photon detector fabricated using the SEG method and performed the study of the timing jitter, which is an important performance parameter of SNSPDs. Our experiment demonstrates an ultrafast YBCO-based photon detector with the rise time ∼850 ps and the fall time ∼1250 ps and a timing jitter of less than ∼100 ps at 810 nm wavelength. Laser power dependence on jitter shows that the minimum value of jitter and small latency are obtained for high incident laser power due to the high rate of hot-spot generation by a large number of absorbed photons. We also present a statistical model of the hot-spot generation to establish the experimental results. Our experimental observations suggest the best reported value of timing jitter for photon detection at a relatively high temperature at 76 K using YBCO as a superconducting microwire.

AUTHOR DECLARATIONS

Conflict of Interest

The authors have no conflicts to disclose.

Author Contributions

A. Kumar and D. Panna contributed equally to this work.

Ankit Kumar: Conceptualization (lead); Data curation (lead); Formal analysis (lead); Investigation (lead); Methodology (lead); Project administration (lead); Resources (lead); Software (lead); Supervision (lead); Validation (lead); Visualization (lead); Writing – original draft (lead); Writing – review & editing (lead). **Dmitry Panna:** Data curation (equal); Formal analysis (equal); Investigation (equal); Methodology (equal); Software (equal); Validation (equal); Visualization (equal); Writing – original draft (equal). **Shlomi Bouscher:** Methodology (supporting); Resources (supporting). **Avi Koriat:** Formal analysis (supporting); Methodology (supporting); Writing – original draft (supporting). **Yuval Nitzav:** Methodology (supporting); Resources (supporting). **Ronen Jacovi:** Methodology (supporting); Resources (supporting). **Amit Kanigel:** Conceptualization (supporting); Funding acquisition (supporting); Investigation (supporting); Project administration (supporting); Resources (supporting); Supervision (supporting); Writing – review & editing (supporting). **Alex Hayat:** Conceptualization (supporting); Formal analysis (supporting); Funding acquisition (supporting); Investigation (supporting); Project administration (supporting); Resources (supporting); Supervision (supporting); Writing – original draft (supporting); Writing – review & editing (supporting).

DATA AVAILABILITY

The data that support the findings of this study are available within the article.

REFERENCES

[1]R. H. Hadfield, "Single-photon detectors for optical quantum information applications," Nat. Photonics **3**, 696–705 (2009).
[2]C. H. Bennett and D. P. DiVincenzo, "Quantum information and computation," Nature **404**, 247–255 (2000).
[3]C. M. Natarajan, M. G. Tanner, and R. H. Hadfield, "Superconducting nanowire single-photon detectors: Physics and applications," Supercond. Sci. Technol. **25**(6), 063001 (2012).
[4]G. G. Taylor, D. Morozov, N. R. Gemmell, K. Erotokritou, S. Miki, H. Terai, and R. H. Hadfield, "Photon counting LIDAR at 2.3 μm wavelength with superconducting nanowires," Opt. Express **27**, 38147–38158 (2019).
[5]N. Zen, A. Casaburi, S. Shiki, K. Suzuki, M. Ejrnaes, R. Cristiano, and M. Ohkubo, "1 mm ultrafast superconducting stripline molecule detector," Appl. Phys. Lett. **95**, 172508 (2009).
[6]A. Cho, "A quantum sensor for dark matter," Science **376**, 448 (2022).
[7]Y. Hochberg, I. Charaev, S. W. Nam, V. Verma, M. Colangelo, and K. K. Berggren, "Detecting sub-GeV dark matter with superconducting nanowires," Phys. Rev. Lett. **123**, 151802 (2019).
[8]G. N. Gol'tsman, O. Okunev, G. Chulkova, A. Lipatov, A. Semenov, K. Smirnov, B. Voronov, A. Dzardanov, C. Williams, and R. Sobolewski, "Picosecond superconducting single-photon optical detector," Appl. Phys. Lett. **79**, 705–707 (2001).
[9]H. Shibata, K. Shimizu, H. Takesue, and Y. Tokura, "Ultimate low system dark-count rate for superconducting nanowire single-photon detector," Opt. Lett. **40**, 3428–3431 (2015).

[10]P. Hu, H. Li, L. You, H. Wang, Y. Xiao, J. Huang, X. Yang, W. Zhang, Z. Wang, and X. Xie, "Detecting single infrared photons toward optimal system detection efficiency," Opt. Express **28**, 36884–36891 (2020).
[11]B. Korzh, Q.-Y. Zhao, J. P. Allmaras, S. Frasca, T. M. Autry, E. A. Bersin, A. D. Beyer, R. M. Briggs, B. Bumble, M. Colangelo *et al.*, "Demonstration of sub-3 ps temporal resolution with a superconducting nanowire single-photon detector," Nat. Photonics **14**, 250–255 (2020).
[12]H. Takesue, S. Nam, Q. Zhang, R. H. Hadfield, T. Honjo, K. Tamaki, and Y. Yamamoto, "Quantum key distribution over a 40-dB channel loss using superconducting single-photon detectors," Nat. Photonics **1**, 343 (2007).
[13]L. You, "Superconducting nanowire single-photon detectors for quantum information," Nanophotonics **9**(9), 2673 (2020).
[14]I. Charaev, D. A. Bandurin, A. T. Bollinger, I. Y. Phinney, I. Drozdov, M. Colangelo, B. A. Butters, T. Taniguchi, K. Watanabe, X. He, O. Medeiros, I. Božović, P. Jarillo-Herrero, and K. K. Berggren, "Single-photon detection using high-temperature superconductors," Nat. Nanotechnol. **18**, 343 (2023).
[15]X. Xing, K. Balasubramanian, S. Bouscher, O. Zohar, Y. Nitzav, A. Kanigel, and A. Hayat, "Photoresponse above 85 K of selective epitaxy grown high-T_c superconducting microwires," Appl. Phys. Lett. **117**, 032602 (2020).
[16]G. Koren, A. Gupta, E. A. Giess, A. Segmüller, and R. B. Laibowitz, "Epitaxial films of $YBa_2Cu_3O_{7-\delta}$ on $NdGaO_3$, $LaGaO_3$, and $SrTiO_3$ substrates deposited by laser ablation," Appl. Phys. Lett. **54**, 1054 (1989).
[17]C. A. J. Damen, H. J. H. Smilde, D. H. A. Blank, and H. Rogalla, "Selective epitaxial growth for YBCO thin films," Supercond. Sci. Technol. **11**, 437 (1998).
[18]J. P. Sydow, M. Berninger, R. A. Buhrman, and B. H. Moeckly, "Effects of oxygen content on YBCO Josephson junction structures," IEEE Trans. Appl. Supercond. **9**, 2993 (1999).
[19]S. Nawaz, T. Bauch, and F. Lombardi, "Transport properties of YBCO nanowires," IEEE Trans. Appl. Supercond. **21**, 164 (2011).
[20]K. Fossheim and A. Sudbø, *Superconductivity: Physics and Application* (John Wiley & Sons, West Sussex, 2005).
[21]P. Tiwari, X. D. Wu, S. R. Foltyn, R. E. Muenchausen, P. N. Arendt, I. H. Campbell, Q. X. Jia, D. E. Peterson, and T. E. Mitchell, "Study of high-quality epitaxial YBCO thin grown directly on Y-Cut $LiNbO_3$," J. Electron. Mater. **25**(1), 131 (1996).
[22]L. Soler, J. Jareño, J. Banchewski, S. Rasi, N. Chamorro, R. Guzman, R. Yáñez, C. Mocuta, S. Ricart, J. Farjas, P. Roura-Grabulosa, X. Obradors, and T. Puig, "Ultrafast transient liquid assisted growth of high current density superconducting films," Nat. Commun. **11**(2), 344 (2020).
[23]Y. V. Cherpak, V. A. Komashko, S. A. Pozigun, A. V. Semenov, C. G. Tretiatchenko, E. A. Pashitskii, and V. M. Pan, "Critical current density of HTS single crystal YBCO thin films in applied dc field," IEEE Trans. Appl. Supercond. **15**, 2783 (2005).
[24]A. Stangl, A. Palau, G. Deutscher, X. Obradors, and T. Puig, "Ultra-high critical current densities of superconducting $YBa_2Cu_3O_{7-\delta}$ thin films in the overdoped state," Sci. Rep. **11**, 8176 (2021).
[25]K. Matsumoto, T. Horide, K. Osamura, M. Mukaida, Y. Yoshida, A. Ichinose, and S. Horii, "Enhancement of critical current density of YBCO films by introduction of artificial pinning centers due to the distributed nano-scaled Y_2O_3 islands on substrates," Physica C **412–414**, 1267 (2004).
[26]A. K. Erlang, "Probability calculation and telephone conversations," Nyt Tidsskrift Matematik B **20**, 33 (1909), https://www.jstor.org/stable/24528622
[27]M. K. Akhlaghi and A. H. Majedi, "Semiempirical modeling of dark count rate and quantum efficiency of superconducting nanowire single-photon detectors," IEEE Trans. Appl. Supercond. **19**(3), 361 (2009).